Rab26 restricts insulin secretion via sequestering Synaptotagmin-1

Ruijuan Zhuang
Xiamen University
Yuxia Zhou
Xiamen University
Ziyan Wang
Xiamen University
Yating Cao
Xiamen University
Liju Xu
Xiamen University
Yandan Ren
Xiamen University
Yige Zheng
Xiamen University
Ziheng Wei
Xiamen University
Jun Chen
Xiamen University
Hantian Qiu
Liangcheng Li
Xiamen University
Yang Han
Institute of Glycobiology, Dalian Medical University, Dalian, Liaoning, China
Ye Yun
Xiamen University
Xin Chen
Xiamen University https://orcid.org/0000-0002-2477-6087
Wanjin Hong
Institute of Molecular and Cell Biology - A-STAR https://orcid.org/0000-0002-1719-8960
Tuanlao Wang (xmuibrwtl@xmu.edu.cn)
Xiamen University https://orcid.org/0000-0001-5375-1615

Article

Keywords: Rab26, Insulin secretion, Synaptotagmin-1, Diabetes

Posted Date: June 14th, 2022

DOI: https://doi.org/10.21203/rs.3.rs-1726613/v1

Abstract

Rab26 is known to regulate multiple membrane trafficking events, but its role in insulin secretion of pancreatic β-cells remains unclear despite it was first identified in the pancreas. In this study, we generated Rab26$^{-/-}$ mice through CRISPR/Cas9 technique. Surprisingly, insulin levels in the blood of the Rab26$^{-/-}$ mice do not decrease upon glucose stimulation, but conversely increases. Deficiency of Rab26 promotes insulin secretion, which was independently verified by Rab26 knockdown in pancreatic β-cells. Conversely, over-expression of Rab26 suppresses insulin secretion in both β-cell lines and isolated mouse islets. Islets over-expressing Rab26, upon transplantation, also failed to restore glucose homeostasis in type 1 diabetic mice. Immuno-fluorescence microscopy revealed that over-expression of Rab26 results in clustering of insulin granules. GST-pulldown experiments reveal Rab26 interacts with synaptotagmin-1(Syt1) through directly binding to its C2A domain. This interaction interferes with the interaction between Syt1 and SNAP25. TIRF microscopy revealed Rab26 inhibits the exocytosis of newcomer insulin granules. Our results suggest that Rab26 serves as a negative regulator of insulin secretion, via suppressing insulin granule fusion with plasma membrane through sequestering Syt1.

Introduction

Insulin is the most important hormone to maintain glucose homeostasis. Defect in insulin secretion is the main pathophysiological mechanism accounting for diabetes mellitus [1]. Islet β cells, a small number of endocrine cells comprising less than 2% of the human pancreas in adults [2], secrete insulin in a biphasic manner in response to secretagogues[3]. Insulin secretion includes a series of vesicular trafficking processes tightly regulated by multiple membrane trafficking machineries such as Rab small GTPases, SNARE proteins and SNARE associated partners. Reduced insulin secretion could be due to either defects in insulin granule transport (granule maturation), docking to or fusion with the plasma membrane, or abnormal degradation of insulin/proinsulin [4, 5, 6].

Rab small GTPases associate with different subcellular compartments of the exocytotic and endocytic pathways [7]. Rab proteins are the key regulators for vesicular trafficking via serving as the molecular switches cycling between GDP-bound and GTP-bound form [8, 9]. GTP-bound form generally engages downstream effectors to regulate vesicle formation and/or tethering or docking. The biogenesis of insulin granules (dense core granules) and insulin secretion are regulated by Rab proteins and their effectors. Two Rab proteins, Rab3 and Rab27 are associated with insulin granules, which interact with multiple effectors to regulate insulin secretion through mediating granule trafficking, docking to the plasma membrane [10]. Especially, mutation in Rab27 caused diabetes in mice [11]. Rab26 was firstly characterized from rat pancreas [12], however, its role in pancreatic β cells remain unclear.

Several studies revealed that Rab26 plays important roles in regulating protein transport. Rab26 is involved in autophagic pathway by regulating autophagic degradation of phosphorylated Src and also linking synaptic vesicles to the autophagy pathway [13, 14]. Rab26 modulates the transport of α2-

adrenergic receptors from the Golgi to the cell surface [15]. Rab26 may also regulate maturation of exocrine granules and may be involved in the recruitment of secretory granules to the plasma membrane to mediate amylase release in rat parotid acinar cells [16]. These studies suggest a potential role of Rab26 in regulating other secretory events such as insulin secretion.

In this study employing Rab26 gene knockout mice, we found that deficiency of Rab26 enhances insulin secretion. Conversely, over-expression of Rab26 inhibits insulin secretion in pancreatic β-cells and freshly isolated mouse islets. Rab26 overexpression induces clustering of insulin granules. Mechanistically, Rab26 interacts with Synaptotagmin-1(Syt1), and this interaction may competitively inhibit Syt1 binding to the SNARE complex to interfere insulin granule fusion to plasma membrane.

Results

Deficiency of Rab26 enhances insulin secretion

Rab26 was firstly identified in rat pancreas [12], and shown to regulate the maturation of exocrine granules to mediate amylase release from rat parotid acinar cells [16]. Rab26 is transcriptionally expressed in multiple tissues, and especially at higher levels in the brain (Figure S1A). To study the physiological role of Rab26, we generated Rab26 gene knockout mice. The whole fragment of Rab26 gene was deleted through CRISPR/Cas9 approach using specific sgRNA targeting to the upstream of exon 1 and downstream of exon 9 of Rab26 gene (Figure 1A). The deletion of fragment was verified by DNA sequencing. The genotypes of mice were assessed by PCR approach (Figure 1B). The homozygous Rab26 gene knock out mice ($Rab26^{-/-}$) were validated not expressing Rab26 as assessed by Western-blot (Figure 1C).

To directly assess the effect of Rab26 deficiency on insulin secretion, we isolated the islets form $Rab26^{-/-}$ mice (as well as control mice), and measured insulin secretion in perfusion culture. Consistently, the fresh islets isolated from $Rab26^{-/-}$ mice secreted much more insulin under 16.7mM glucose stimulation as compared to control islets (Figure 1D and 1E), suggesting that absence of Rab26 promotes insulin secretion from islets to increase the circulating levels of insulin in response to glucose.

To further support our conclusion, we depleted Rab26 in mouse pancreatic β-cells through CRISPR/Cas9 technique (Figure 1F). The stable INS-1 cell line with Rab26 depleted was used to examine insulin secretion. As shown in Figure 1G, depletion of Rab26 significantly increased insulin secretion. These results support the conclusion that deficiency of Rab26 enhances insulin secretion.

Deficiency of Rab26 in mice improves glucose homeostasis

Insulin is the most important hormone for regulating glucose homeostasis, therefore, we examined the effects of depletion of Rab26 on glucose tolerance in mice. We first performed intraperitoneal Glucose Tolerance Test (IPGTT) to assess the consequence of Rab26 depletion. As shown in Fig 1H and 1I, $Rab26^{-/-}$ mice have higher insulin levels in the blood upon glucose stimulation than wild type (WT)

mice. And the glucose level in the plasma of Rab26$^{-/-}$ mice is much lower than that of WT mice under normal feeding condition (Figure 1J and 1K). The body weight of Rab26$^{-/-}$ mice is less than that of WT mice (Figure S1B). Intraperitoneal insulin tolerance tests (IPITT) demonstrated that Rab26$^{-/-}$ is more sensitive to insulin (Figure 1L and 1M), since the blood glucose levels lowered down faster in Rab26$^{-/-}$ mice. Together with the above results, deficiency of Rab26 may improve glucose homeostasis to prevent diabetes development through enhanced insulin secretion.

Over-expression of Rab26 restricts insulin secretion in β-cells

As depletion of Rab26 enhanced insulin secretion, we did the converse experiment to show that over-expression of Rab26 inhibits insulin secretion. Pancreatic β-cells MIN6 or INS-1 were infected with the recombinant adenovirus expressing Rab26 (Ad-Rab26) (Figure S2A and S2B), and then insulin secretion was detected by ELISA assay. As shown in Figure 2A-D, insulin secretion was clearly suppressed in both MIN6 (Figure 2A) and INS-1 (Figure 2C) cells upon overexpressing Rab26 in response to glucose stimulation, corresponding AUCs of insulin release stimulated by 16.7 mM glucose was decreased in MIN6 (Figure 2B) and INS-1 (Figure 2D) cells. In addition, the biphasic secretion pattern was disrupted in Ad-Rab26 infected MIN6 or INS-1 cells. However, the transcripts of Ins1 and Ins2 genes were not altered by expression of Rab26 (Figure S2C).

To examine whether the inhibitory effects of Rab26 is dependent of its guanine nucleotide binding activity, INS-1 cells were infected with Ad-Rab26, Ad-Rab26T77N (dominant negative mutant prefers binding to GDP), Ad-Rab26Q123L (constitutive active mutant with GTPase activity inhibited) or Ad-vector (Figure S2D). Cells were stimulated by glucose, then insulin secretion was detected by ELISA assay. The results demonstrated that insulin secretion was significantly suppressed by Ad-Rab26 or Ad-Rab26Q123L, but not by Ad-Rab26T66N (Figure 2E), suggesting the inhibitory effect of Rab26 on insulin secretion is physiologically regulated by its guanine nucleotide binding activity.

GLP-1 is a glucose-dependent hormone stimulating insulin secretion [17], we investigated the effect of Rab26 on GLP-1 stimulated insulin secretion, the results indicated that GLP-1 indeed enhanced insulin secretion. Importantly, Rab26 also suppressed GLP-1 stimulated insulin secretion (Figure 2F), indicating Rab26 restricts the glucose-stimulated insulin secretion (GSIS) in pancreatic β-cells.

As mentioned above, depletion of Rab26 enhancing insulin secretion in INS-1 cells. A rescue experiment revealed that insulin secretion was reduced upon replenishing Rab26 by infection of Ad-Rab26 in Rab26-knockout INS-1 (Figure 2G). Taken together, our results suggest that Rab26 serves as a negative regulator to restrict insulin secretion in pancreatic β-cells and this regulation is dependent on its guanine nucleotide binding activity.

The pathophysiological relevance of Rab26 to diabetes mellitus

To further define the role of Rab26 in insulin secretion, freshly isolated mouse islets were effectively infected with Ad-Rab26 (Figure 3A). Insulin secretion from islets was stimulated by 16.7mM glucose

in KRBH buffer, as shown in Figure 3B, over-expression of Rab26 significantly inhibited insulin secretion from islets at different detection time points compared with islets transduced with vector control, suggesting over-expression of Rab26 suppresses insulin secretion not only in β-cell lines, but also in freshly isolated islets which is close to the in vivo physiological condition.

Next, we examined whether Rab26 affected the function of islets in vivo. The mouse model of type 1 diabetes was established by intraperitoneal injection of streptozotocin to destroy the islets (Figure 3C). Immunofluorescence staining with insulin antibody showed that injection of streptozotocin destroyed the islets accompanied with high blood glucose levels, indicating that the model of type 1 diabetic mice was generated (Figure 3D). Islets infected with Ad-Rab26 or vector were transplanted back to type 1 diabetes mice beneath the renal capsule (Figure 3E). The transplanted mice were intraperitoneally injected with glucose, then the plasma insulin and blood glucose were monitored. As expected, the plasma insulin levels of type 1 diabetic mice transplanted with islets overexpressing Rab26 were much lower than that of control mice (Figure 3F). Meanwhile, the blood glucose levels of mice transplanted with islets overexpressing Rab26 decreased more slowly and kept at high level for longer period of time (continuously monitored for 6 days, Figure 3G, 3H). The mice transplanted with Ad-Rab26 islets exhibits hyperglycemia with glucose levels up to 25 mM, while the glucose levels of control mice were restored to normal (Figure 3G, 3H). The results suggest that overexpression of Rab26 not only restricted insulin secretion but also suppressed the rescuing function of isolated islets upon transplantation into type I diabetic experimental model.

Since Rab26 is involved in insulin secretion, the expression of Rab26 may be related to diabetes mellitus. Immuno-histochemistry analysis found the staining signals of Rab26 in islet of db/db mice are stronger than that of WT mice (Figure 3I), indicating high levels of Rab26 protein in islets of db/db mice. Furthermore, Rab26 protein level was elevated under high glucose or high palmitic acid conditions (Figure 3J, 3K). These results suggest that the expression of Rab26 is closely related diabetic pathophysiological conditions.

Rab26 associates with insulin granules and regulates the distribution of insulin granules

To investigate how Rab26 regulates insulin secretion, we examined the subcellular location of Rab26 and the effects of its over-expression on the distribution of insulin granules in β-cells. Rab26 was shown to be associated with the endocytic compartments [18]. Immuno-fluorescence microscopy revealed GFP-Rab26 was present in puncta which co-localized with pro (insulin) and Vamp4 in MIN6 cells (Figure 4A), suggesting Rab26 associates with the secretory vesicles and insulin granules. Further examinations demonstrated that Rab26 associates with insulin-labeled granules (Figure 4B). In addition, over-expression of Rab26 resulted in insulin granules clustering in normal media, KRB buffer containing 2.8 mM glucose or 16.7 mM glucose in MIN6 cells (Figure 4B). Under normal conditions, over-expression of Rab26WT or Rab26Q123L mutant induced insulin granules clustering, while the inactivated mutant Rab26T77N was distributed in the cytosol and didn't induce insulin granule granules clustering (Figure 4C). Consistent with the results that Rab26WT and Rab26Q123L but not Rab26T77N inhibit insulin

secretion, this clustering distribution of insulin granules induced by Rab26 may inhibit glucose stimulation triggered exocytosis of insulin granules and consequently restrict insulin secretion.

Rab26 interacts with synaptotagmin-1

To uncover the molecular mechanism for Rab26 in regulating insulin secretion, we searched for its interacting proteins. Synaptotagmin-1(Syt1) along with several other proteins were identified as potential interacting partners of Rab26 from rat brain tissue lysate in large scale GST-pulldown experiments (Figure S3A). Syt1 is an important calcium sensor to regulate neurotransmitter release in neuron and insulin secretion in pancreatic β-cells [19, 20]. The interaction of Rab26 with Syt1 was validated by analytic GST-pulldown assay. The interaction between Rab26 and Syt1 depends on Rab26's nucleotide binding activity, as the interaction between GDP-bound mutant Rab26T77N and Syt1 was dramatically reduced (Figure 5A). In vitro binding assay using prokaryotic-expressed GST-Syt1 and His-Rab26 showed Rab26 can directly bind to Syt1 (Figure 5B). In addition, GST-pulldown experiments using GST-Rab26 revealed that Rab26 only interacts with Syt1-C2A domain, but not C2B domain in cell lysates derived from cells transfected with GFP-Syt1, GFP-Syt1-C2A or GFP-Syt1-C2B (Figure 5C), suggesting Rab26 binds directly Syt1 through interacting with the C2A domain in a manner dependent on its binding with GTP (Figure 5D). Besides Syt1, other members of Synaptotagmin such as Syt4 and Syt7 may regulate insulin secretion as well [21, 22]. However, Rab26 did not interact with either Syt4 or Syt7 (Figure S3C), suggesting Rab26 specifically interacts with Syt1.

The interaction between Rab26 and Syt1 is essential to its inhibitory activity for insulin secretion

To investigate whether Rab26 restricts insulin secretion through interaction with Syt1, we first examined whether Rab26 associates with Syt1 at insulin granules. Immuno-fluorescence microscopy revealed that Rab26 is co-localized with Syt1 and insulin (Figure 5E). GFP-Rab26 also induced Syt1-containing insulin granules clustering in MIN6 cells under normal culture condition or glucose stimulation. These results imply Rab26 can associate with insulin granules by binding to Syt1, and consequently regulates exocytosis of insulin granules.

Over-expression of Syt1 promotes insulin secretion [23]. We prepared Lentivirus-mediated over-expression of Syt1 in INS-1 cells, the cells then were infected with Ad-Rab26 (Figure 6A). Insulin secretion was monitored by ELISA assay. Indeed, over-expression of Syt1 enhanced insulin secretion in INS-1 cells (Figure 6B). However, insulin secretion enhanced by Syt1 was significantly suppressed when Ad-Rab26 was co-expressed with Syt1 (Figure 6B), suggesting Rab26 inhibits insulin secretion through interaction with Syt1.

By examining Genbank, we found that Rab26 gene encodes another shorter isoform (accession No. NM_001308053.1) referred to as Rab26b [24]. Rab26b protein lacks N-terminal 66 amino acids. Interestingly, Rab26b was not able to interact with Syt1 in GST-pulldown experiments (Figure 6C), which was verified by using GST-Rab26 or GST-Rab26b to bind GFP-Syt1 (Figure S3B). In addition, Rab26b was not recruited to Syt1 containing insulin granules and was distributed primarily in the cytosol, not inducing

granules clustering either (Figure 6D). As expected, over-expression of Rab26b had no significant inhibitory effects on glucose-stimulated insulin secretion in both INS-1 and MIN6 cells (Figure 6E, 6F). These results suggest N-terminal extension of Rab26 as compared to Rab26b is necessary for interaction with Syt1, clustering insulin granules or restricting insulin secretion. Taken together, these results suggest that Rab26 restricts insulin secretion via interacting directly with C2A region of Syt1 in a manner that is dependent on the N-terminal region and GTP-bound status of Rab26.

Rab26 influences the interaction between Syt1 and SNARE complex

Since Syt1 facilitates secretory vesicles docking to and fusion with plasma membrane through interaction with SNARE complex [25], we next examined whether Rab26 influences the interaction between Syt1 and SNARE complex. 293t cells were co-transfected with myc-Rab26 and GFP-SNAP25 or GFP-Syntaxin-1, the cell lysates were subjected for GST-pulldown using GST-Syt1. As shown in Figure 7A and 7B, the amount of SNAP25 protein bound to GST-Syt1 was significantly reduced in cells expressing Rab26 compared with control vector. However, expression of Rab26 had no effects on Syt1 binding to Syntaxin-1 (Figure 7C and 7D). Ca^{2+} stimulation promoted Syt1 binding to SNAP25, which was inhibited by Rab26 expression (Figure 7E and 7F). These results suggest that interaction of Rab26 with Syt1 inhibits Syt1 binding to SNAP25. Rab26 thus may restrict insulin secretion via sequestering Syn1 from interacting with SNAP-25.

As Syt1 can bind to phospholipids, we investigated whether Rab26 interaction with Syt1 influences Syt1 binding to phospholipids. In vitro overlay assay revealed that Rab26 did not affect the interaction of Syt1 with $PI(4,5)P_2$ and PS (Figure S4). Therefore, Rab26 inhibits insulin secretory granules exocytosis probably by interfering Syt1 interaction with SNARE complex, and consequently inhibit insulin secretory granules fusion with the plasma membrane.

Rab26 inhibits exocytosis of newcomer insulin granules

Rab26 inhibits SNAP25 binding to Syt1, suggesting that Rab26 may influence Syt1 interaction with SNARE complex and consequently insulin secretory granules (ISGs) fusion with the plasma membrane. To examine this hypothesis, MIN6 cells were co-transfected with GFP-Rab26 and DsRed-Insulin, and then analyzed for the ISGs dynamics by employing time-lapse total internal reflection fluorescence microscopy (TIRFM).

The exocytotic events were, however, not uniform but could be categorized into three distinct modes of exocytosis. Pre-dock SGs that were visible before stimulation, no-dock newcomers SGs that fused without remaining at the plasma membrane for ≤ 200 milliseconds (interval of one frame), and short-dock newcomers SGs that appeared during stimulation and stably remained for > 200 milliseconds before fusion occurs. The number of pre-docked SGs was counted and averaged at the first 2 min prior to stimulation. At unstimulated state, the average number of pre-docked ISGs in Rab26-transfected cells is similar to that of vector-transfected cells (Figure 8A), when stimulated with 16.7mM glucose (containing GLP-1 and IBMX), the accumulated fusion events in Rab26-transfected cells were significantly less than

that in vector-transfected cells (Figure 8B). Single SG fusion dynamic analysis revealed that no fusion events were observed before stimulation. Both the newcomer SGs no-dock and newcomer SGs short-dock were decreased in Rab26-transfected cells compared to that in vector-transfected cells, and not displaying two-phase secretion pattern in Rab26-transfected cells (Figure 8C), which is consistent with the results shown in Figure 2A and 2B. The fusion events summarized from newcomer no-dock SGs and newcomer SGs short-dock demonstrated Rab26 significantly inhibits the newcomer SGs fusion with the plasma membrane (Figure 8D). Taken together, Rab26 interaction with Syt1 may interfere Syt1 interaction with SNARE complex and consequently inhibit ISGs exocytosis, resulting in the inhibition of insulin secretion.

Discussion

Rab26 is implicated in multiple vesicular trafficking events, such as autophagy, exocrine granule release, synaptic vesicle trafficking and mitochondrial distribution [14, 26, 27]. Our earlier study showing RILP is involved in insulin secretion [18] prompted us to investigate the role of Rab26 in insulin secretion. In this study, we generated Rab26 gene knockout mice, and found deficiency of Rab26 enhances insulin secretion and improves glucose homeostasis in diabetic mice, suggesting its role in restricting insulin secretion. Consistently, Rab26 protein level in islets of diabetic mice is elevated, as well as under high glucose or fatty acid conditions.

Rab26 is a transcriptional target of MIST1 that regulates the formation of exocrine secretory granules in human gastric cancer cell [28]. Our results showed that depletion of Rab26 promotes insulin secretion in mice or pancreatic β-cells, while over-expression of Rab26 inhibits insulin secretion in both beta cell lines and freshly isolated islets. These findings suggest Rab26 exerts a different function in regulating secretory pathway in pancreatic β-cells. Coincidently, RILP (Rab7-interacting lysosomal protein) also restricts insulin secretion through mediating proinsulin degradation [18]. By contrary, Rab3 and Rab27 positively regulate insulin secretion [10, 29], indicating insulin secretion is tightly regulated by diverse mechanisms to maintain its homeostasis.

More than 10 members of Synaptotagmin family were identified, and several of them have been established to regulate Ca^{2+} triggered insulin granules exocytosis [22, 23, 30, 31]. Synaptotagmin-1 (Syt1) is the most important Ca^{2+} sensor in regulating insulin secretion in pancreatic β-cells [20, 32]. Syt1 has two regulatory domains C2A and C2B, which interact with SNARE (soluble NSF associated protein receptor) SNAP25/Syntaxin1/Vamp, as well as phosphatidylinositol-(4,5) bisphosphate on the plasma membrane, thus mediating Ca $^{2+}$ triggered secretory vesicles docking and fusion with plasma membrane [33, 34, 35, 36, 37]. Mechanistically, Rab26 directly binds to the C2A domain of Syt1. We also demonstrated that Rab26-Syt1 interaction is essential to Rab26's inhibitory activity on insulin secretion, as an isoform Rab26b not interacting with Syt1 doesn't inhibit insulin secretion. Although Syt1 may interact with SNARE SNAP25 and Syntaxin1, in our study, over-expression of Rab26 only specifically interferes the interaction between

Syt1 and SNAP25, suggesting SNAP25 and Syntaxin-1 may bind to the different region or motifs of Syt1, which deserves further examination.

Syt1 interaction with SNARE may help SNARE complex clamping or zippering [38, 39]. In addition, Syt1 binds to PI(4,5)P_2 to help insulin granule docking [40, 41]. Nevertheless, the precise mechanisms for Syt1 regulating exocytosis remains to be elucidated. C2B domain of Syt1 seems more flexible to interact with accessary partners, however, there is some cooperation between C2A and C2B, and they can influence each other [42, 43]. Therefore, Rab26 interaction with C2A domain may influence the function of C2B. Although we presented data indicating the interaction between Rab26 and Syt1 influences SNARE complex formation, more precise details need to be worked in future studies. Therefore, Rab26 interacting with C2A domain of Syt1 will sequester it from promoting the formation of SNARE complex involved in the docking and fusion of insulin granules (Fig. 8E).

Rab26's interaction with Syt1, its role in clustering of insulin granules, and its inhibition on insulin secretion are all dependent on its GTP-bound state as the wild-type, GTP-bound mutant but not GDP-restricted mutant displayed these effects. Collectively, these results suggest that Rab26 restricts insulin secretion via sequestering Syt1 on insulin granule to suppress the docking and fusion. This conclusion raises the interesting possibilities that proteins regulating GTP cycle of Rab26 such as its GEFs and GAPs are likely involved in regulating insulin secretion. These candidate GEFs and GAPs may receive other physiological inputs so that insulin secretion is precisely regulated, although their identities remain to be identified.

To maintain insulin balance, excess subcellular insulin may be channeled to degradation pathway [44, 45]. RILP mediates lysosomal degradation of proinsulin, which also interacts with Rab26 [18]. Rab26 also mediates autophagic pathway [13, 14]. As Rab26 restricts insulin granules exocytosis, the accumulated/clustered insulin granules may potentially be directed to degradation through the above mentioned degradation pathway to maintain insulin homeostasis.

In summary, our results uncover a novel function of Rab26 which negatively regulates insulin secretion in pancreatic β-cells. Mechanistically, Rab26 interacts with Syt1 to interfere SNAP25-Syt1 interaction, consequently influencing insulin granule docking and fusion with plasma membrane.

Materials And Methods

Generation of Rab26 gene knockout mice

C57BL/6J mouse strain was used for generating gene knock-out model. Rab26 gene knockout mice were generated using CRISPR/Cas9 approach. sgRNA-1 (5-GACCCGAACCCGTCCCGCAGCGG-3) and sgRNA-2 (5-TAGACTCGGGCAATTCTCAAAGG-3) targeting to the flanking region 5' of exon 1 and 3' of last exon of Rab26 gene, respectively, were used to delete the whole genomic region encoding Rab26 in mouse embryonic stem cells. The genotypes of mice were verified by tail DNA PCR using specific forward primer

1 (5-GACAACTGGAGCCCTTTGAG-3), reverse primer 2 (5-GGCCTTGCAGTAGATGGAGT-3) and mutant reverser primer 3 (5-GACGGTATCAGCGCATGTGT-3) and Western-blot assay using Rab26 antibody.

Cell culture and transfection

MIN6, INS-1, 293T and 293A cell lines were from ATCC (American Type Culture Collection). MIN6 cells were maintained in Dulbecco's modified Eagle's medium (DMEM, Invitrogen, cat. No.12800017) supplemented with 10% FBS and 50μM β-Mercaptoethanol in 5% CO2 incubator at 37°C. INS-1 cells were maintained in RPMI-1640 supplemented with 10% FBS, 10 mM Hepes, 1 mM PyrNa and 50μM β-Mercaptoethanol in 5% CO2 incubator at 37°C. Cells were transfected by using Lipofactamine2000 reagents (Invitrogen) according to the manufacturer's protocol.

Antibodies and Reagents

Rab26 rabbit monoclonal antibody (mAb) was purchased from Proteintech (cat.14284-1AP). Rabbit polyclonal antibody against insulin (cat. no. 4590 s) was from Cell Signaling Technology. Proinsulin mAb was obtained from HyTest (cat. no. CCI-17). mAb against α-tubulin (cat.66031-1-Ig) and GFP (cat.66002-1-Ig) were from Proteintech (Wuhan, China). mAb against syt1 was purchased from Synaptic Systems (cat. no.105011). mAb against Myc (9E10) was obtained from American Type Culture Collection (ATCC, Manassas, VA, USA). HRP-conjugated secondary antibodies, Cy5-conjugated, Texas red-conjugated were from Jackson Immuno Research (cat. 111-035-003, 115-025-003, 111-175-144, 115-295-003, West Grove, PA, USA). GLP-1(Glucagon-like peptide-1) and IBMX (Isobutyl-1-methylxanthine) was purchased from MCE (MedChemExpress). Collagenase V, STZ (Streptozotocin) and PA (Palmitic Acid) were purchased from Sigma-Aldrich.

Expression plasmids and Virus-mediated gene expression

GFP-Rab26WT, GFP-Rab26Q123L, GFP-Rab26T77N, myc-Rab26, GST-Rab26WT, GST-Rab26Q123L, GST-Rab26T77N, GFP-Rab26b and GST-Rab26b were described previously [18]. Synaptotagmin-1 (Syt1) cDNA was retrieved from mouse cDNA. GFP-Syt1, GFP-Syt1C2A (1-263aa), GFP-Syt1C2B (264-422aa) were constructed by subcloning the correspondent coding region into pEGFP-C1 vector, respectively. GST-tagged Syt1or its truncated mutant plasmids were generated by subcloning the correspondent coding region into pGEX- 4T-1 vector, respectively. His-Rab26 and DsRed-preproinsulin was contructed by similar method into pet-28a and pDSred-N1 plasmid. GFP-SNAP25 and GFP-Syntaxin1A were from Wanjin Hong's Laboratory (Institute of Molecular and Cell Biology, Singapore).

Adenovirus was produced as described [46]. Briefly, Rab26WT, Rab26Q123L and Rab26T77N coding regions were cloned into pAdTrack-CMV vector. The plasmids were then linearized and transformed into the competent AdEasier E. coli cells to generate recombinant adenovirus plasmid. The recombinant adenovirus plasmids were transfected into 293A cells to produce recombinant adenovirus (referred as Ad-Rab26 etc.).

Over-expression of Syt1 was achieved by pCDH-CMV-MCS-EF1-Puro vector mediated lentivirus expression system. For virus preparation, 293T cells were transfected with lentiviral skeleton and helper plasmids (pMD2.G, psPAX2) for 48 h, and the culture medium was collected. In case of virus infection, the cells were inoculated on a 6-well plate, 1 ml of lentivirus stock solution was added after 24h, and fresh culture medium was changed for 12h. The expression level of the target protein was detected by Western blot.

CRISPR/Cas9 mediated gene knockout

Rab26-deficient INS-1 cells were generated using CRISPR/Cas9 system as described [18]. sgRNA-1 sequence (5-GTCCTGGGATGTGCCAGACG-3) and sgRNA-2 sequence (5- GAGGGCCGGCCGGACTGCGG -3) were used to disrupt the expression of Rab26 in INS-1 cells. The disruption of Rab26 gene was verified by genomic DNA sequencing and Western-blot.

Detection of insulin secretion

MIN6 and INS-1 cells were infected with adenovirus. Cells were pre-incubated with Krebs-Ringer bicarbonate buffer (KRBH containing 114 mM NaCl, 4.7 mM KCl, 1.2 mM KH_2PO_4, 1.16 mM $MgSO_4$, 0.5 mM $MgCl_2$, 2.5 mM $CaCl_2$, 0.25% BSA and 20 mM HEPES, pH 7.4) containing 2.8 mM glucose for 60 min, followed by incubation in 2.0 ml of stimulation medium (KRBH containing 16.7 mM glucose). Insulin secretion were detected by ELISA kits (ImmunoDiagnostics Limited, China) at different time points as described [47].

For detection of insulin secretion from islets, islets were isolated from mouse pancreas as described [48], the freshly isolated islets or adenovirus-infected islets were applied for perfusion culture under glucose stimulation, the media was collected for insulin measurement by ELISA kits (ImmunoDiagnostics Limited, China) as described above.

Animal experiments

The body weight of mice was monitored every week and the blood glucose level was determined by an Accu-Chek glucose meter (Roche Diagnostics). For insulin tolerance tests (ITTs), fasting mice were intraperitoneally injected with 0.75 units of insulin (Gansulin R) per kg body weight, and blood glucose was measured at the designated time points. Intraperitoneal Glucose Tolerance Test (IPGTT) were performed via intraperitoneal injection of 2.0 g/kg glucose into mice after fasting for 16h as described [49]. Blood samples were taken from the tail vein at the indicated time points.

Type 1 diabetic mice were generated as described [50]. Briefly, mice were intraperitoneally injected with 70mg/kg streptozotocin (STZ) for 5 days. After a week, the blood glucose level of mice was randomly monitored and mice with a blood glucose levels up to 16.7 mM showed that the model of type 1 diabetes (T1DM) was successfully constructed as described [50]. The diabetic mice were transplanted with the freshly isolated islets. About 300 islets infected by Ad-Rab26 or Ad-vector were suspended in 20 µl RPMI

medium containing 10% FBS. Then the virus infected islets were transplanted into the renal capsule of mice as described [51]. IPGTT was generated as described above.

Mice were exposed to light / dark cycle for 12 hours at room temperature and sufficient food and water. And Rab26$^{-/-}$ mice were bred by heterozygosity and maintained in the Xiamen University Laboratory Animal Center. BKS db/db diabetic mice were obtained from Model Animals Research Center of Nanjing University (#T002407, BKS-lepr^{em2Cd479}/Nju). All animal experiments were conducted in strict accordance with the guiding principles of experimental animals in the regulations of Institutional Animal Ethics Committee of Xiamen University.

Immunofluorescence microscopy

Immuno-staining was performed as previously described [52]. Briefly, cells grown on coverslips were washed with PBSCM (PBS containing 1.0mM CaCl2 and 1.0mM MgCl2) for 10 minutes three times, and then fixed with 4% paraformaldehyde at room temperature for 20min. After three times of PBSCM washing, cells were permeabilized with 0.1% Triton-100 (Sigma) in PBSCM for 10min at room temperature.

For tissue staining, the islets were cryosectioned, and the cryosections were permeabilized with 0.2% Triton X-100 and then blocked with 0.2% BSA and subjected for immuno-staining using the primary antibodies, followed by fluorophone-conjugated secondary antibodies. The immuno-labeled cells or tissues were analyzed with Carl Zeiss LSM7 EXITER or Leica TCS SP8 STED laser scanning confocal microscope.

Immuno-histological chemistry

Pancreatic tissue was immunohistochemical stained to detect the expression profile of Rab26 according the manufacturer's protocol. Briefly, the paraffin-embedded pancreatic tissues were cut at a 4-μm thickness. Deparaffinized and rehydrated, then processed for antigen recovery. After blocking with 3% BSA for 30 min at room temperature, and then incubated with Rab26 antibody and treated with HRP (horseradish peroxidase) conjugated secondary antibody (ZSGB-BIO, cat.No.PV-9001), then incubated with DAB for color development. The tissue was observed under microscope (Olympus BX53).

GST pulldown assay and Western blot

GST-pulldown assay was applied for detection of protein-protein interaction. Briefly, cells transfected with the indicated plasmids were lysed in binding buffer (containing 20mM Hepes, pH 7.4, 1% Triton-100, 100mM NaCl, 5mM MgCl2, and EDTA-free proteinase inhibitor cocktail from Roche) for 1h on ice. The cell lysates were clarified by spinning at 14000 rpm for 30min.The supernatants were incubated with GST-fusion protein coupled to GST-Sepharose 4B resin (GE healthcare, cat. No. 45-000-139) at 4°C for 4 hours. The proteins bound to GST sepharose beads were detected through Western blot assay.

Western-blot was performed as described [53]. Briefly, cells were lysed in RIPA buffer containing proteinase inhibitor cocktail (Roche, cat.No. 04693132001). The resulted cell lysates were separated by SDS-PAGE, the resolved proteins were transferred to PVDF membrane, then the membrane was blocked with 5% milk in TBST, followed by incubation with primary antibodies and HRP- conjugated secondary antibody. The blots were detected using ECL system (Pierce, Rockford, IL, USA).

TIRF Microscopy and data analysis

MIN6 cells were co-transfected with DsRed-preproinsulin and Vector or GFP-Rab26 for 24 hours, respectively. Before image acquisition, the cells were pre-incubated for 30 minutes in KRB buffer containing 2.8 mM glucose. The microscope is equipped with a temperature control device and a carbon dioxide device to keep the experiment at 37°C with 5% carbon dioxide. The cells were incubated with 2.8mM glucose for 2 minutes, then 2.8mM glucose containing 10nM GLP-1 and 150μM IBMX (Isobutyl-1-methylxanthine) for 3 minutes, and finally stimulated with 16.7mM glucose containing 10nM GLP-1 and 150μM IBMX for 18 minutes.

Time-lapse TIRF microscopy was performed on a Nikon Ti-E inverted microscope using a 100 x oil immersion TIRF objective (NA 1.49). We used an Agilent MLC-400B laser launch with 488 nm and 568 nm solid-state lasers to excite EGFP and DsRed, respectively. The fluorescence signals were detected by an electron-multiplying charge-coupled device camera (EMCCD) under the control of NIS-Elements AR software. TIRF images were acquired at 5-Hz with an exposure time of 100 ms. SGs were localized, counted and analyzed using ImageJ and Imaris.

Fusion events, observed as flashes of fluorescence indicating emptying of DsRed-preproinsulin cargo, were manually selected, as recently reported in detail [54]. An increase of DsRed fluorescence exceeding five times over the standard deviation of the fluorescence fluctuation was considered as fusion events. We used a concentric circle (~7 pixels with a pixel size of 160 nm, corresponding to approximately 1.12 μm diameter) to center on the selected SGs to characterize the evolution of fluorescence over time of single SGs on background-subtracted images. Fusion events were also indicated by abrupt brightening of fluorescence, and were manually selected for analyses of SGs exocytosis.

Statistical analysis

The data were presented as mean ± standard deviation (SD) with GraphPad Prism 7.0. Statistical significance between two groups was assessed using Student's t-tests or among multiple groups using two-way ANOVA. A value of $P<0.05$ was indicated as statistical significance.

Declarations

Acknowledgement

This work was supported by National Natural Science Foundation of China (No. 31871423, 9195411182000741, 32160207, 31871386 and 32070736).

Author contribution

ZR involved in data analysis and contributed to Figure 1, 2, 5, 6, 7 and S4. ZY involved in data analysis and contributed to Figure 1, 3, 4 and S1. WZ contributed to Figure 1, 2. XL contributed to Figure 5. RY contributed to Figure 7. LL involved in data analysis. CJ contributed to Figure S2. QH contributed to Figure S3. YY and HY provided technical support. CX contributed to TIRFM and data analysis. HW involved in the ideas discussion and paper writing. WT conceived the idea for the project, experiments design, data analysis and wrote the paper.

Ethics statement

All animal experiments were approved by Institutional Animal Ethics Committee of Xiamen University, China.

Funding statement

National Natural Science Foundation of China: project No. 31871423, 91954111□82000741, 32160207, 31871386 and 32070736.

Conflict of interest:

The authors declare that they have no conflicts of interest with this work.

Data and Resource Availability

Data and resource are available from the corresponding authors.

Guarantor's statement

Dr. Tuanlao Wang is the guarantor of this work and, as such, had full access to all the data in the study and takes responsibility for the integrity of the data and the accuracy of the data analysis.

References

1. Ashcroft FM, Rorsman P. Diabetes mellitus and the beta cell: the last ten years. Cell 2012, **148**(6): 1160–1171.
2. Houtz J, Borden P, Ceasrine A, Minichiello L, Kuruvilla R. Neurotrophin Signaling Is Required for Glucose-Induced Insulin Secretion. Developmental Cell 2016, **39**(3): 329–345.
3. Kalwat MA, Cobb MH. Mechanisms of the amplifying pathway of insulin secretion in the beta cell. Pharmacol Ther 2017, **179**: 17–30.

4. Nguyen PM, Gandasi NR, Xie B, Sugahara S, Xu Y, Idevall-Hagren O. The PI(4)P phosphatase Sac2 controls insulin granule docking and release. J Cell Biol 2019, **218**(11): 3714–3729.
5. Omar-Hmeadi M, Idevall-Hagren O. Insulin granule biogenesis and exocytosis. Cell Mol Life Sci 2021, **78**(5): 1957–1970.
6. Hou JC, Min L, Pessin JE. Insulin granule biogenesis, trafficking and exocytosis. Vitam Horm 2009, **80**: 473–506.
7. Lang T, Jahn R. Core proteins of the secretory machinery. Handb Exp Pharmacol 2008(184): 107–127.
8. Barr F, Lambright DG. Rab GEFs and GAPs. Curr Opin Cell Biol 2010, **22**(4): 461–470.
9. Muller MP, Goody RS. Molecular control of Rab activity by GEFs, GAPs and GDI. Small GTPases 2018, **9**(1–2): 5–21.
10. Cazares VA, Subramani A, Saldate JJ, Hoerauf W, Stuenkel EL. Distinct actions of Rab3 and Rab27 GTPases on late stages of exocytosis of insulin. Traffic 2014, **15**(9): 997–1015.
11. Kowluru A. A lack of 'glue' misplaces Rab27A to cause islet dysfunction in diabetes. J Pathol 2016, **238**(3): 375–377.
12. Wagner AC, Strowski MZ, Goke B, Williams JA. Molecular cloning of a new member of the Rab protein family, Rab 26, from rat pancreas. Biochem Biophys Res Commun 1995, **207**(3): 950–956.
13. Dong W, He B, Qian H, Liu Q, Wang D, Li J, *et al.* RAB26-dependent autophagy protects adherens junctional integrity in acute lung injury. Autophagy 2018, **14**(10): 1677–1692.
14. Binotti B, Pavlos NJ, Riedel D, Wenzel D, Vorbruggen G, Schalk AM, *et al.* The GTPase Rab26 links synaptic vesicles to the autophagy pathway. Elife 2015, **4**: e05597.
15. Li C, Fan Y, Lan TH, Lambert NA, Wu G. Rab26 modulates the cell surface transport of alpha2-adrenergic receptors from the Golgi. J Biol Chem 2012, **287**(51): 42784–42794.
16. Nashida T, Imai A, Shimomura H. Relation of Rab26 to the amylase release from rat parotid acinar cells. Arch Oral Biol 2006, **51**(2): 89–95.
17. Wu B, Wei S, Petersen N, Ali Y, Wang X, Bacaj T, *et al.* Synaptotagmin-7 phosphorylation mediates GLP-1-dependent potentiation of insulin secretion from beta-cells. Proc Natl Acad Sci U S A 2015, **112**(32): 9996–10001.
18. Zhou Y, Liu Z, Zhang S, Zhuang R, Liu H, Liu X, *et al.* RILP Restricts Insulin Secretion Through Mediating Lysosomal Degradation of Proinsulin. Diabetes 2020, **69**(1): 67–82.
19. Xu J, Mashimo T, Sudhof TC. Synaptotagmin-1, -2, and – 9: Ca(2+) sensors for fast release that specify distinct presynaptic properties in subsets of neurons. Neuron 2007, **54**(4): 567–581.
20. Nakajima-Nagata N, Sugai M, Sakurai T, Miyazaki J, Tabata Y, Shimizu A. Pdx-1 enables insulin secretion by regulating synaptotagmin 1 gene expression. Biochem Biophys Res Commun 2004, **318**(3): 631–635.
21. Huang C, Walker EM, Dadi PK, Hu R, Xu Y, Zhang W, *et al.* Synaptotagmin 4 Regulates Pancreatic beta Cell Maturation by Modulating the Ca(2+) Sensitivity of Insulin Secretion Vesicles. Dev Cell

2018, **45**(3): 347–361 e345.

22. Dolai S, Xie L, Zhu D, Liang T, Qin T, Xie H, *et al.* Synaptotagmin-7 Functions to Replenish Insulin Granules for Exocytosis in Human Islet beta-Cells. Diabetes 2016, **65**(7): 1962–1976.
23. Gauthier BR, Wollheim CB. Synaptotagmins bind calcium to release insulin. Am J Physiol Endocrinol Metab 2008, **295**(6): E1279-1286.
24. Liu H, Zhou Y, Qiu H, Zhuang R, Han Y, Liu X, *et al.* Rab26 suppresses migration and invasion of breast cancer cells through mediating autophagic degradation of phosphorylated Src. Cell Death Dis 2021, **12**(4): 284.
25. Ullah N, Maaiden EE, Uddin MS, Ashraf GM. Synaptotagmin-1: A Multi-Functional Protein that Mediates Vesicle Docking, Priming, and Fusion. Curr Protein Pept Sci 2021.
26. Yoshie S, Imai A, Nashida T, Shimomura H. Expression, characterization, and localization of Rab26, a low molecular weight GTP-binding protein, in the rat parotid gland. Histochem Cell Biol 2000, **113**(4): 259–263.
27. Jin RU, Mills JC. RAB26 coordinates lysosome traffic and mitochondrial localization. J Cell Sci 2014, **127**(Pt 5): 1018–1032.
28. Tian X, Jin RU, Bredemeyer AJ, Oates EJ, Blazewska KM, McKenna CE, *et al.* RAB26 and RAB3D are direct transcriptional targets of MIST1 that regulate exocrine granule maturation. Mol Cell Biol 2010, **30**(5): 1269–1284.
29. Yi Z, Yokota H, Torii S, Aoki T, Hosaka M, Zhao S, *et al.* The Rab27a/Granuphilin Complex Regulates the Exocytosis of Insulin-Containing Dense-Core Granules. Molecular and Cellular Biology 2002, **22**(6): 1858–1867.
30. Iezzi M, Kouri G, Fukuda M, Wollheim CB. Synaptotagmin V and IX isoforms control Ca2+ -dependent insulin exocytosis. J Cell Sci 2004, **117**(Pt 15): 3119–3127.
31. Gao Z, Reavey-Cantwell J, Young RA, Jegier P, Wolf BA. Synaptotagmin III/VII isoforms mediate Ca2+-induced insulin secretion in pancreatic islet beta -cells. J Biol Chem 2000, **275**(46): 36079–36085.
32. Xiong X, Zhou KM, Wu ZX, Xu T. Silence of synaptotagmin I in INS-1 cells inhibits fast exocytosis and fast endocytosis. Biochem Biophys Res Commun 2006, **347**(1): 76–82.
33. Robinson IM, Ranjan R, Schwarz TL. Synaptotagmins I and IV promote transmitter release independently of Ca(2+) binding in the C(2)A domain. Nature 2002, **418**(6895): 336–340.
34. Perin MS, Fried VA, Mignery GA, Jahn R, Sudhof TC. Phospholipid binding by a synaptic vesicle protein homologous to the regulatory region of protein kinase C. Nature 1990, **345**(6272): 260–263.
35. Lang J, Fukuda M, Zhang H, Mikoshiba K, Wollheim CB. The first C2 domain of synaptotagmin is required for exocytosis of insulin from pancreatic beta-cells: action of synaptotagmin at low micromolar calcium. EMBO J 1997, **16**(19): 5837–5846.
36. Martens S, Kozlov MM, McMahon HT. How synaptotagmin promotes membrane fusion. Science 2007, **316**(5828): 1205–1208.

37. Earles CA, Bai J, Wang P, Chapman ER. The tandem C2 domains of synaptotagmin contain redundant Ca2 + binding sites that cooperate to engage t-SNAREs and trigger exocytosis. J Cell Biol 2001, **154**(6): 1117–1123.
38. Wang Z, Liu H, Gu Y, Chapman ER. Reconstituted synaptotagmin I mediates vesicle docking, priming, and fusion. J Cell Biol 2011, **195**(7): 1159–1170.
39. Houy S, Groffen AJ, Ziomkiewicz I, Verhage M, Pinheiro PS, Sorensen JB. Doc2B acts as a calcium sensor for vesicle priming requiring synaptotagmin-1, Munc13-2 and SNAREs. *Elife* 2017, **6**.
40. Bai J, Tucker WC, Chapman ER. PIP2 increases the speed of response of synaptotagmin and steers its membrane-penetration activity toward the plasma membrane. Nat Struct Mol Biol 2004, **11**(1): 36–44.
41. van den Bogaart G, Meyenberg K, Diederichsen U, Jahn R. Phosphatidylinositol 4,5-bisphosphate increases Ca2 + affinity of synaptotagmin-1 by 40-fold. J Biol Chem 2012, **287**(20): 16447–16453.
42. Mackler JM, Drummond JA, Loewen CA, Robinson IM, Reist NE. The C(2)B Ca(2+)-binding motif of synaptotagmin is required for synaptic transmission in vivo. Nature 2002, **418**(6895): 340–344.
43. Fernandez I, Arac D, Ubach J, Gerber SH, Shin O, Gao Y, *et al.* Three-dimensional structure of the synaptotagmin 1 C2B-domain: synaptotagmin 1 as a phospholipid binding machine. Neuron 2001, **32**(6): 1057–1069.
44. Ebato C, Uchida T, Arakawa M, Komatsu M, Ueno T, Komiya K, *et al.* Autophagy is important in islet homeostasis and compensatory increase of beta cell mass in response to high-fat diet. Cell Metab 2008, **8**(4): 325–332.
45. Saltiel AR. Insulin Signaling in the Control of Glucose and Lipid Homeostasis. Handb Exp Pharmacol 2016, **233**: 51–71.
46. Luo J, Deng ZL, Luo X, Tang N, Song WX, Chen J, *et al.* A protocol for rapid generation of recombinant adenoviruses using the AdEasy system. Nat Protoc 2007, **2**(5): 1236–1247.
47. Pan Y, Hui X, Hoo RLC, Ye D, Chan CYC, Feng T, *et al.* Adipocyte-secreted exosomal microRNA-34a inhibits M2 macrophage polarization to promote obesity-induced adipose inflammation. J Clin Invest 2019, **129**(2): 834–849.
48. Huang C, Gu G. Effective Isolation of Functional Islets from Neonatal Mouse Pancreas. *J Vis Exp* 2017(119).
49. Zhai K, Gu L, Yang Z, Mao Y, Jin M, Chang Y, *et al.* RNA-binding protein CUGBP1 regulates insulin secretion via activation of phosphodiesterase 3B in mice. Diabetologia 2016, **59**(9): 1959–1967.
50. Fujita I, Utoh R, Yamamoto M, Okano T, Yamato M. The liver surface as a favorable site for islet cell sheet transplantation in type 1 diabetes model mice. Regen Ther 2018, **8**: 65–72.
51. Brissova M, Fowler M, Wiebe P, Shostak A, Shiota M, Radhika A, *et al.* Intraislet endothelial cells contribute to revascularization of transplanted pancreatic islets. Diabetes 2004, **53**(5): 1318–1325.
52. Wang TL, Zhang M, Ma ZX, Guo K, Tergaonkar V, Zeng Q, *et al.* A role of Rab7 in stabilizing EGFR-Her2 and in sustaining Akt survival signal. Journal of Cellular Physiology 2012, **227**(6): 2788–2797.

53. Wang Z, Zhou Y, Hu X, Chen W, Lin X, Sun L, *et al.* RILP suppresses invasion of breast cancer cells by modulating the activity of RalA through interaction with RalGDS. Cell Death Dis 2015, **6**: e1923.

54. Zhu D, Koo E, Kwan E, Kang Y, Park S, Xie H, *et al.* Syntaxin-3 regulates newcomer insulin granule exocytosis and compound fusion in pancreatic beta cells. Diabetologia 2013, **56**(2): 359–369.

Figures

Figure 1

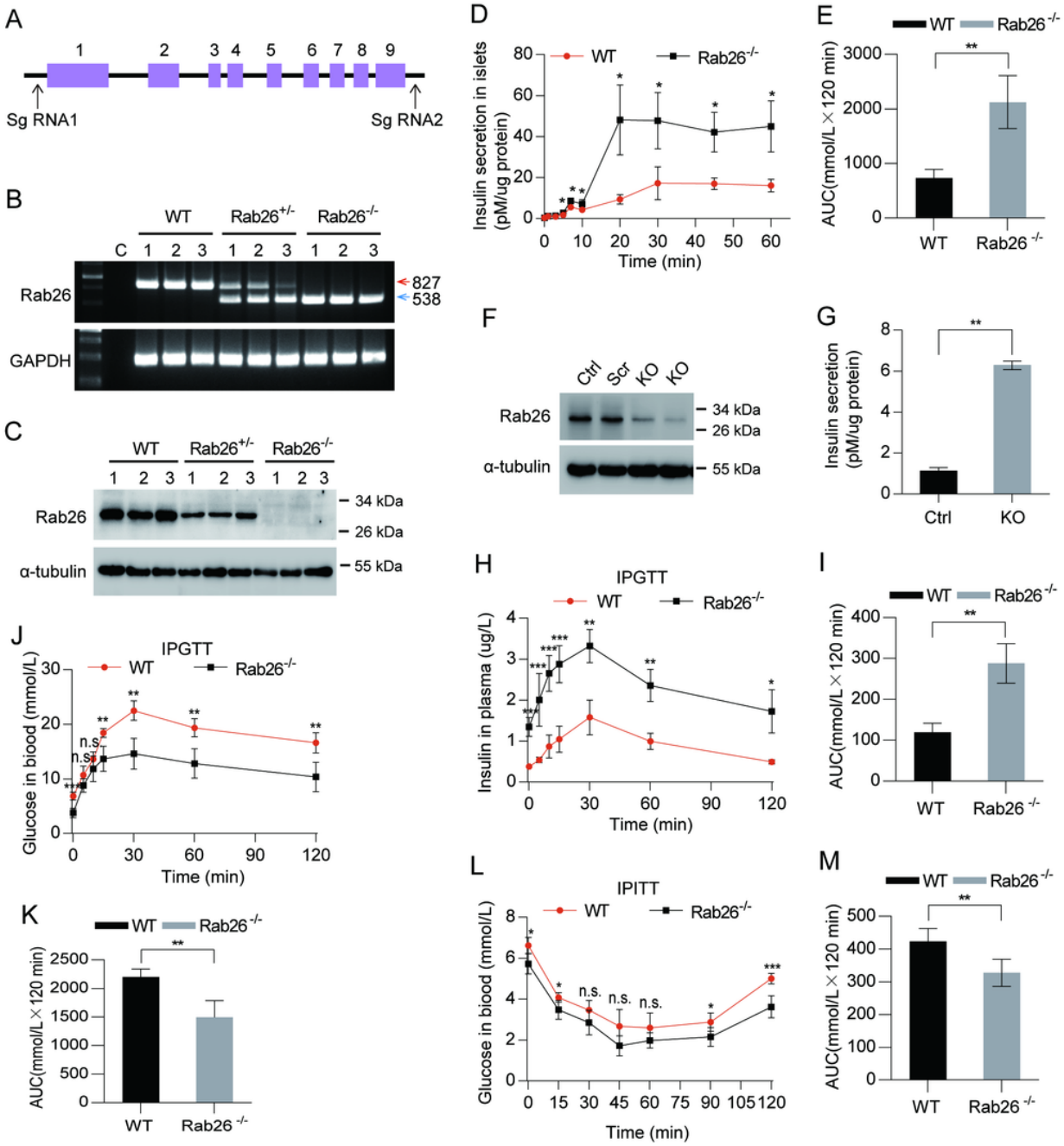

Figure 1

Deficiency of Rab26 enhances insulin secretion. (A), Gene-trap strategy for generating Rab26 knockout (KO) mice. (B), PCR products were used to identify mouse tail DNA to confirm Rab26 gene deletion. Wild types (WT) exhibit 827bp fragments, heterozygous mutant mice produced 827bp and 538bp fragments, and homozygous mutant mice produced 538bp fragments from genomic DNA, respectively. (C), Western-blot using lysates of pancreas isolated from 8-week-old WT, Rab26 $^{+/-}$ and Rab26 $^{-/-}$ mice showed the depletion of Rab26. α-tubulin was used as a loading control. IPGTT and IPITT were performed in Rab26 $^{-/-}$ mice. (D), 100 fresh mouse islets with uniform size were isolated and cultured in 1640 medium containing 10% FBS. The insulin secretion of mouse islets was detected by ELISA at the appointed time. (E), And AUC were calculated. (F), The Rab26 knockout INS-1 cell lines were generated by CRISPR/Cas9 technique, Western-blot detection showed the depletion of Rab26. (G), insulin secretion in Rab26 knockout INS-1 cells. (H), Plasma insulin levels and (I), AUC for glucose during the IPGTT. The IPGTT was performed in mice before (overnight fast) and 2 h after glucose injected intraperitoneally. (J), Blood glucose levels and (K), AUC for glucose during the IGPTT. (L) and (M), WT or KO mice were fasted for overnight before glucose levels were measured in the morning. For the ITT, blood glucose levels and AUC were measured after insulin injected intraperitoneally. (n = 3-9 per group; NS, not significant, ***P < 0.001, **P < 0.01, *P < 0.05, t-tests)

Figure 2

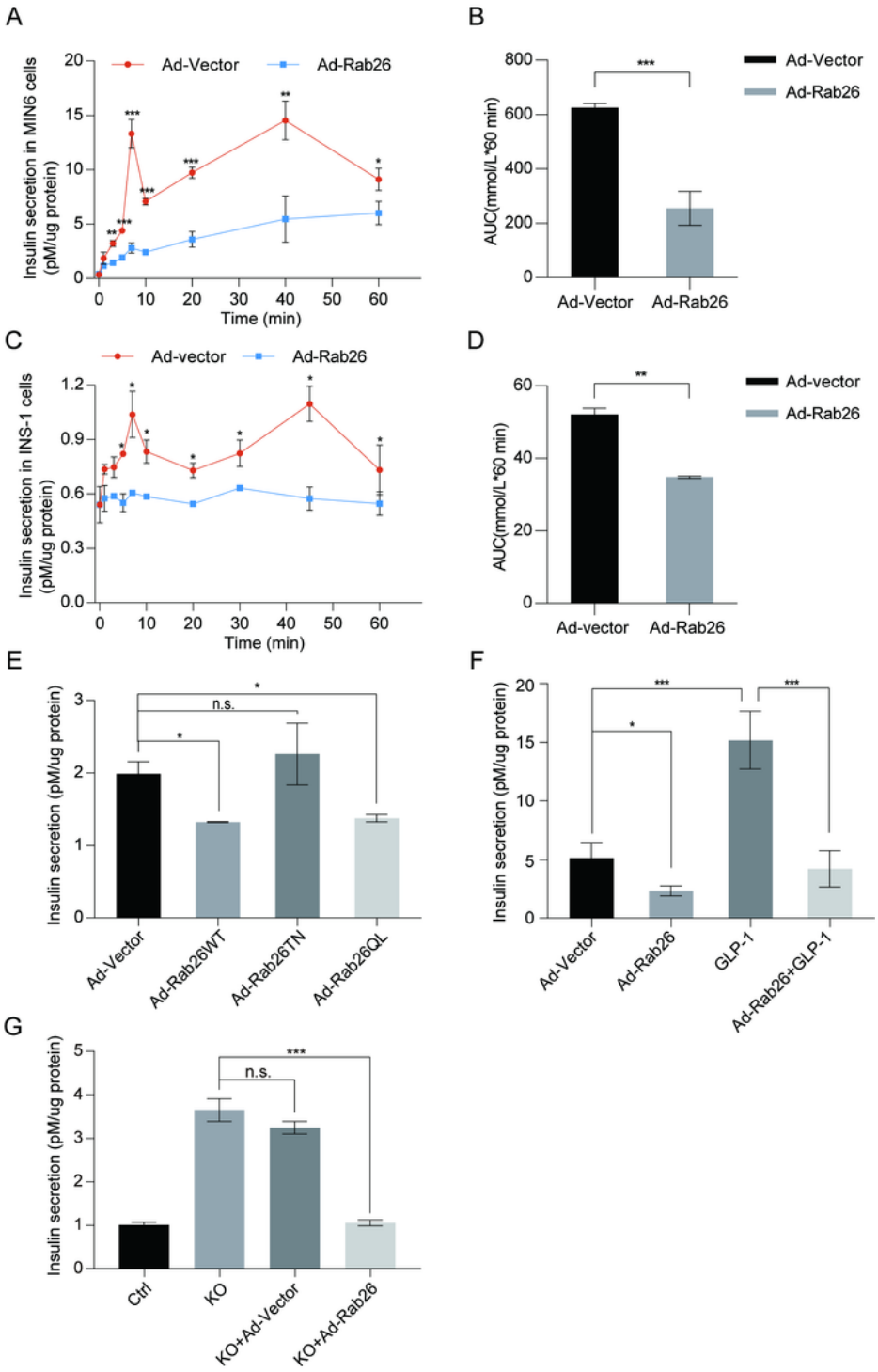

Figure 2

Over-expression of Rab26 restricts insulin secretion in β-cells. (A-DB), MIN6 cells (A) and INS-1 cells (C) were infected with Ad-Rab26, after 40h, cells were balanced with 2.8mM glucose in KRBH buffer for 1h, then stimulated with 16.7mM glucose in KRBH buffer for at different time points. Supernatant insulin secretion was measured by ELISA, corresponding AUCs (area under the curve) of MIN6 (B) or INS-1 (D) cells insulin release stimulated by 16.7 mM glucose stimulated. (E), INS-1 cells were infected with Ad-

Rab26WT, Ad-Rab26T77N, Ad-Rab26Q123L and Ad-vector, balanced with 2.8mM glucose in KRBH buffer for 1h, then stimulated with 16.7mM glucose in KRBH buffer for 30min. Supernatant insulin secretion was measured by ELISA. (F), INS-1 cells were transfected with Ad-vector and Ad-Rab26 alone or co-cultured with 10nM GLP-1. Supernatant insulin secretion was measured by ELISA. (G), Compared with the control, the insulin secretion of KO increased significantly, then in KO monoclonal cell line infected with Ad-Vector and Ad-Rab26, ELISA showed that Rab26 decreased insulin secretion under GSIS condition. (n=3; NS, not significant, ***P < 0.001, **P < 0.01, *P < 0.05, t-tests)

Figure 3

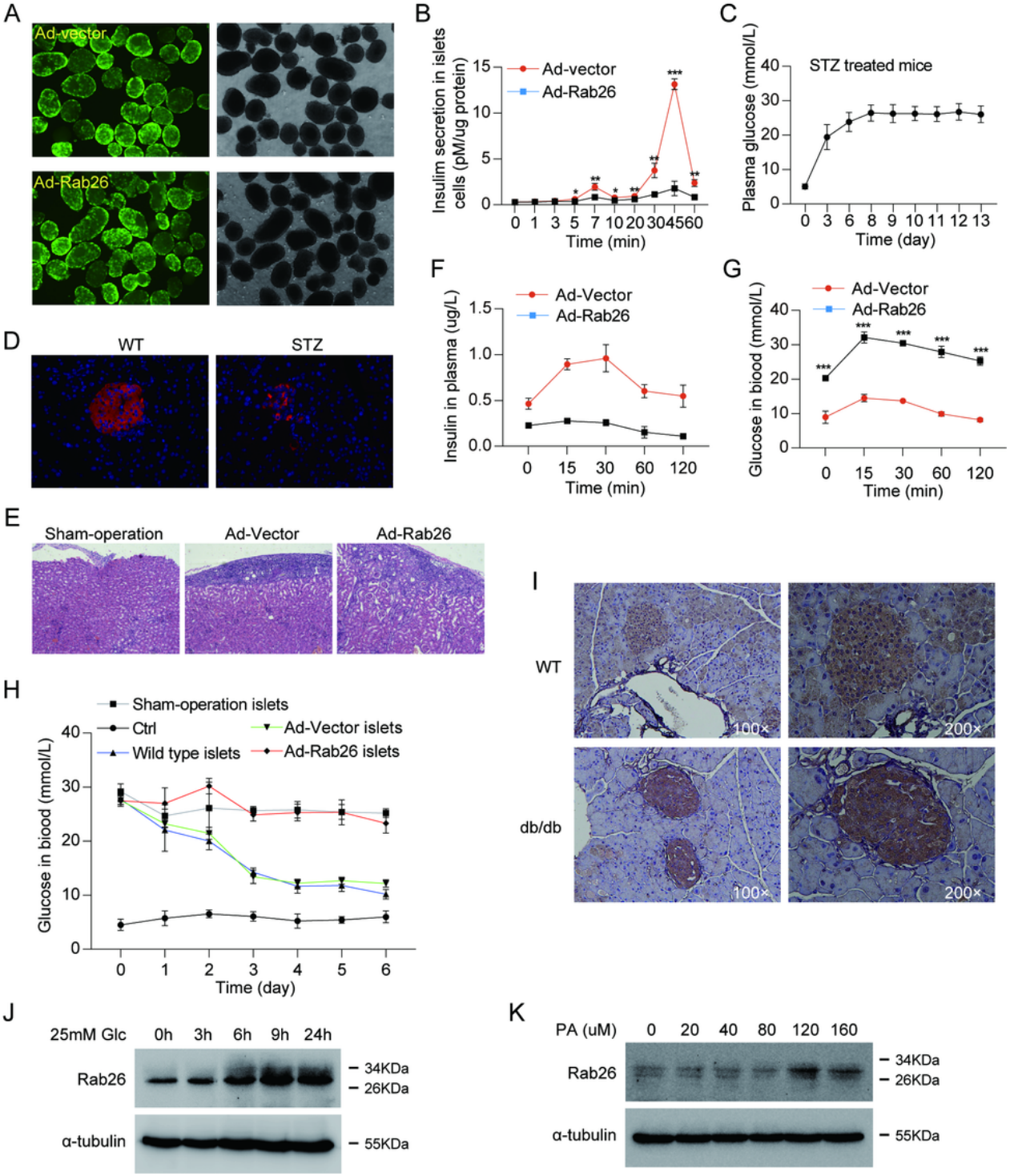

Figure 3

The pathophysiological relevance of Rab26 to diabetes mellitus. (A), Fresh mouse islets were isolated and cultured in 1640 medium containing 10% FBS. 100 islets of uniform size were selected and infected with Ad-Rab26 and Ad-vector, (B) then insulin secretion of mouse islets assessed by ELISA at the indicated time. (C), After intraperitoneal injection of streptozotocin, the blood glucose of 20-22g male C57BL/6J mice increased. (D), Normal mouse islets (left panel) and injected streptozotocin mice islets (right panel), insulin antibody immunofluorescence staining showed that the right islets were destroyed, indicating that the model of type 1 diabetic mice was successful. (E), H&E staining of mice renal capsule performed with islets transplantation. (F), The islets infected by Ad-Rab26 were transplanted into type 1 diabetic mice. In IPGTT experiment, the level of plasma insulin in mice was detected at 0min, 15min, 30min, 60min, and 120min time points after transplantation for 5 days. (G), And blood glucose levels were measured from tail vein. (H), Compared with normal mice, the blood glucose of type 1 diabetic mice with islet transplantation decreased, but the blood glucose of mice infected with Ad-Rab26 could not be reduced within 6 days after transplantation of islets. (I), Representative immunohistochemical images indicating Rab26 protein expression in WT and *db/db* mice pancreas. The images were performed with 5 mice pancreas in each of the 2 groups. (J), Western blot showed that Rab26 protein expression increased after 25 mM glucose stimulation for different time. (K), Western blot showed that Rab26 protein expression increased after PA stimulation for different concentration. (n=3-5; NS, not significant, ***P < 0.001, **P < 0.01, *P < 0.05, t-tests)

Figure 4

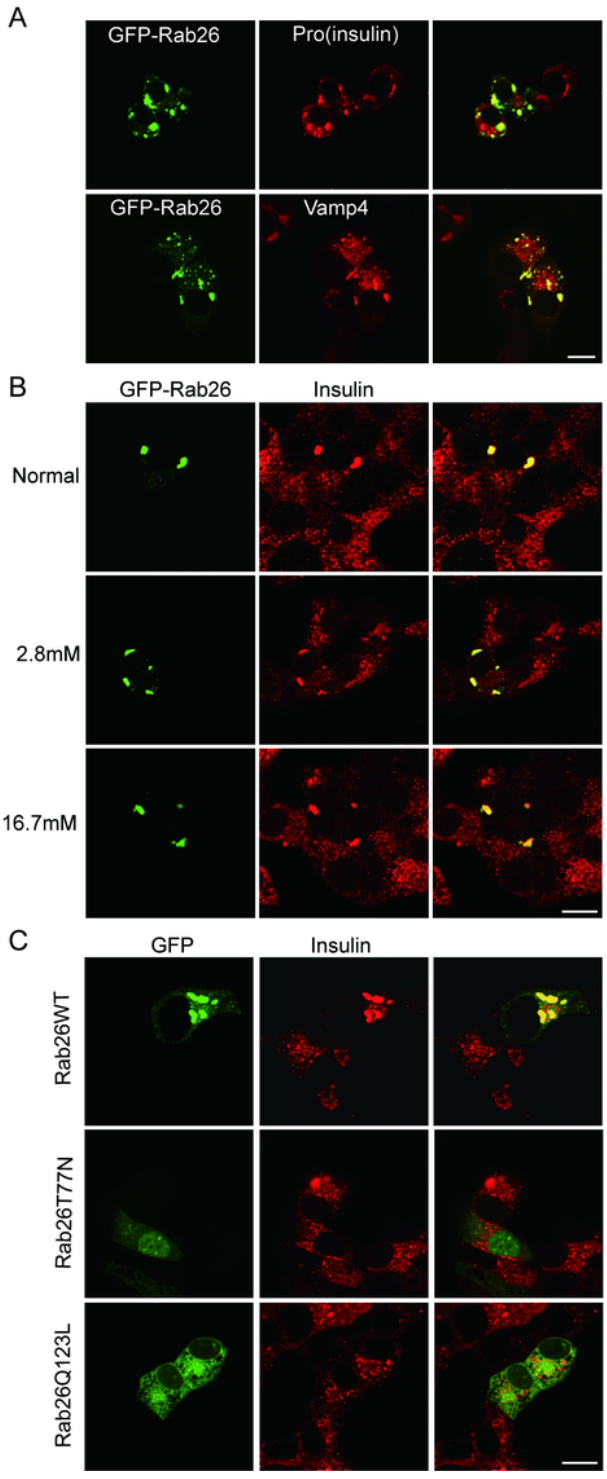

Figure 4

Rab26 induces clustering and enlargement of insulin particles. (A), MIN6 cells transfected with GFP-Rab26 were cultured in KRB buffer containing 16.7mM glucose for 40min, and immuno-fluorescence microscopy revealed GFP-Rab26 was expressed in puncta which co-localized with pro(insulin) and Vamp4. (B), In MIN6 cells transiently transfected plasmids, insulin were similarly dispersed throughout

the cytosol and displayed a similar extent of co-localization with Rab26WT. (C), MIN6 cells were transfected with GFP-Rab26WT, Rab26T77N or Rab26Q123L, and labeled with insulin. Bar=20μm.

Figure 5

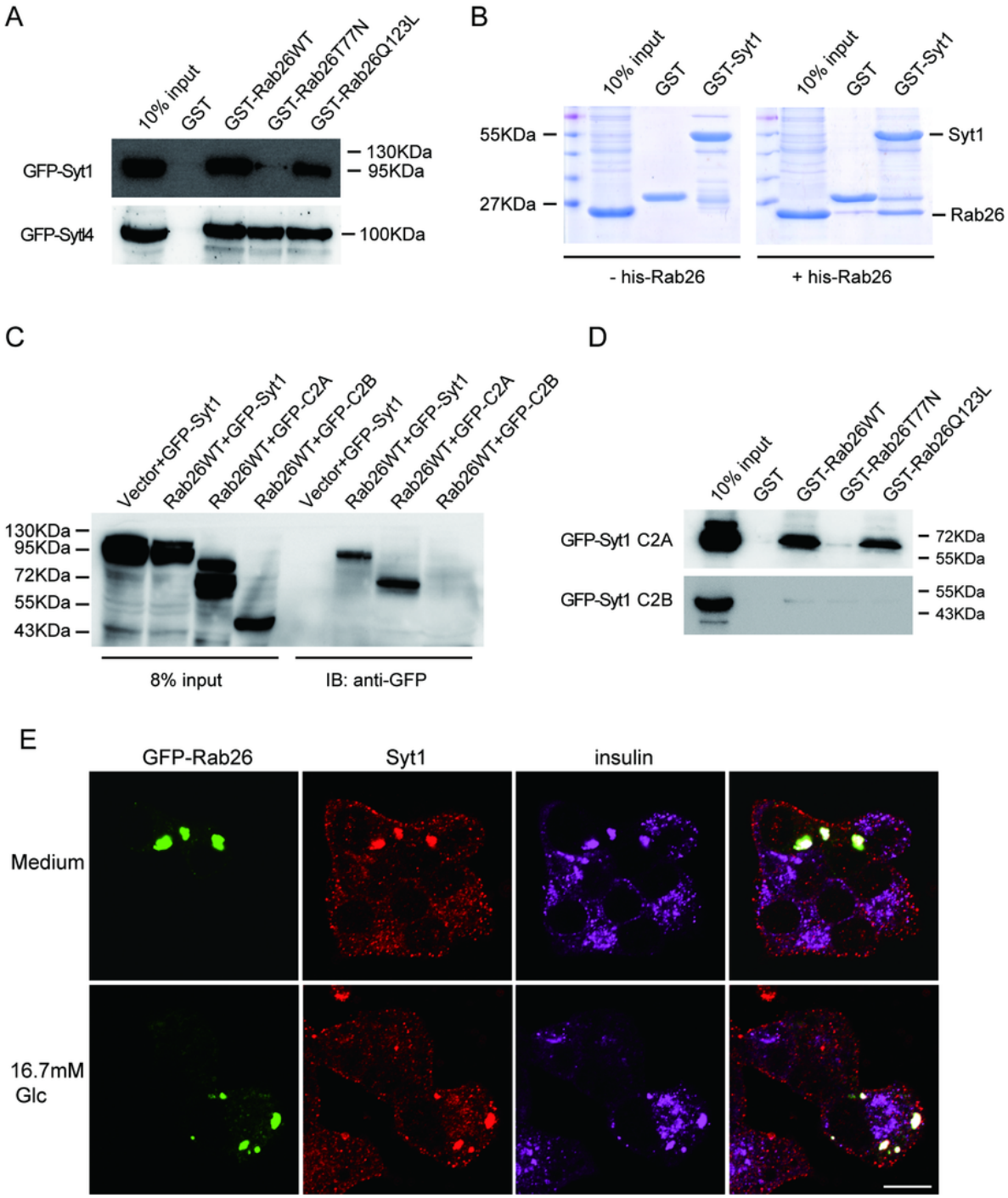

Figure 5

Rab26 directly interacts with Syt1. (A), GST, GST-Rab26WT, GST-Rab26T77N and GST-Rab26Q123L were mixed with the lysate of transiently transfected GFP-Syt1 cells in 293T cells, respectively. Western blotting

analysis was performed with GFP antibody. (B), In vitro binding assay showed His-Rab26 can directly bind to GST-Syt1. (C), GFP-Syt1 and GST-Vector, GFP-Syt1 and GST-Rab26, GFP-Syt1-C2A and GST-Rab26, GFP-Syt1-C2B and GST-Rab26, cell lysate was mixed, and after extensive washing. After a large number of washing, Western blotting analysis was performed with GFP antibody. (D), GST, GST-Rab26WT, GST-Rab26TN and GST-Rab26QL were mixed with the lysate of transient transfection of GFP-Syt1 or GFP-Syt1-C2B domain in 293T cells, respectively. After a large amount of washing, Western blotting analysis was performed with GFP antibody. (E), MIN6 cells transfected with GFP-Rab26 were cultured in normal medium or in KRB buffer containing 16.7mM glucose for 40min, and then immuno-stained with antibody against Syt1 and insulin, showing Rab26 induces Syt1 and insulin granules clustering. Bar=20μm

Figure 6

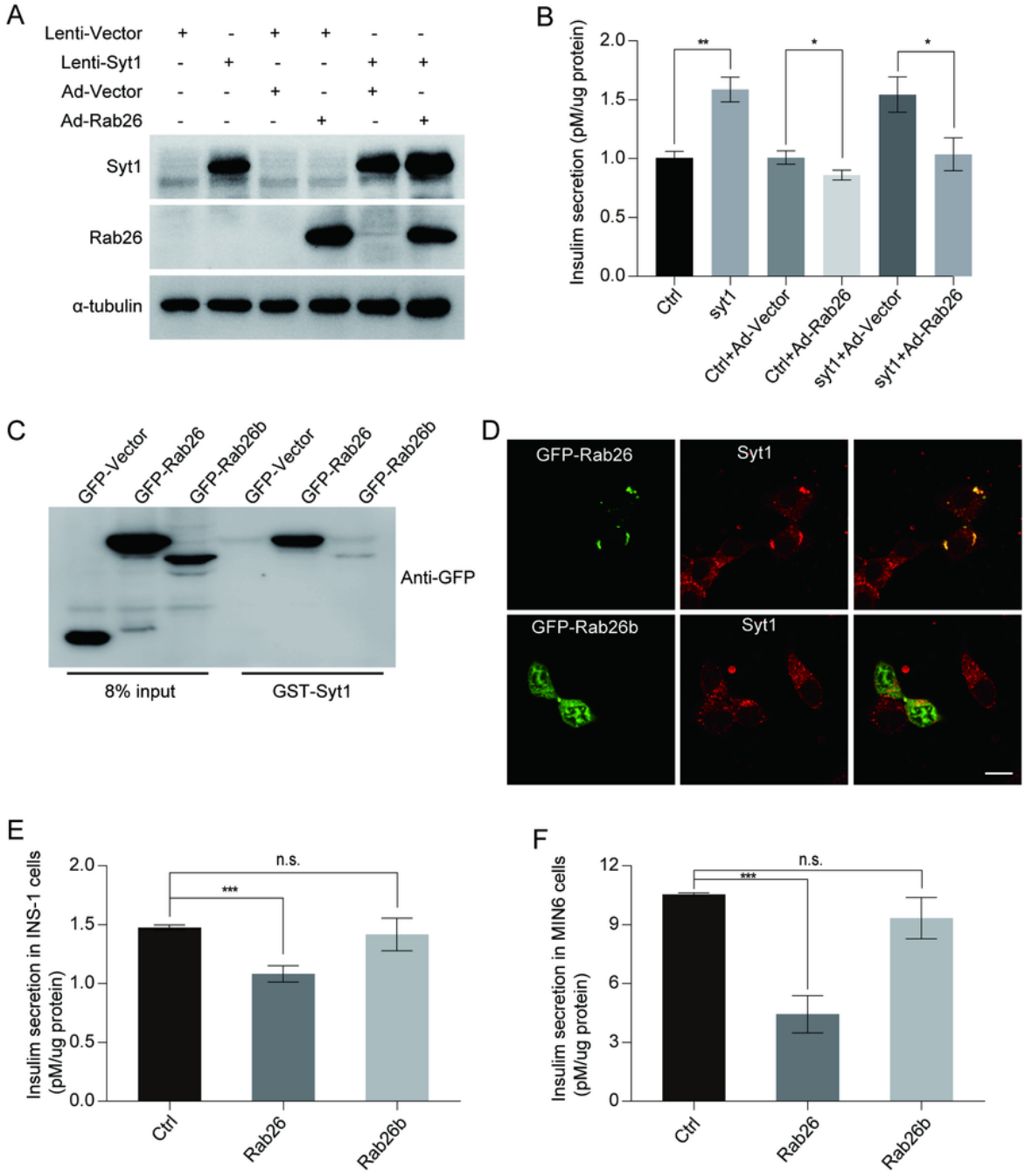

Figure 6

The interaction between Rab26 and Syt1 is essential to its inhibitory activity for insulin secretion. (A) and (B), INS-1 cells were infected with lenti-syt1, then infected with Ad-Rab26, the corresponding cells were stimulated for insulin secretion in KRBH buffer under GSIS condition, insulin secretion were assessed by ELISA, and Western-blot was used to detect Syt1, Rab26 and α-tubulin. (C), 293t cells were transfected GFP-Vector, GFP-Rab26 or GFP-Rab26b, and the derived cells lysates were incubated overnight with GST-

syt1 beads at 4°C through GST-pull down experiment. (D), MIN6 cells transfected with GFP-Rab26 or GFP-Rab26b were cultured in normal medium, and then immuno-stained with antibody against Syt1. (E), and (F), INS-1 cells and MIN6 cells were infected with the Ad-vector, Ad-Rab26 or Ad-Rab26b, after 48h, and balanced in KRBH buffer with 2.8mM glucose for 1h, then stimulated with glucose(16.7mM) for 30min. Insulin secretion was assessed by ELISA. (n=3-5; NS, not significant, ***P < 0.001, **P < 0.01, *P < 0.05, t-tests)

Figure 7

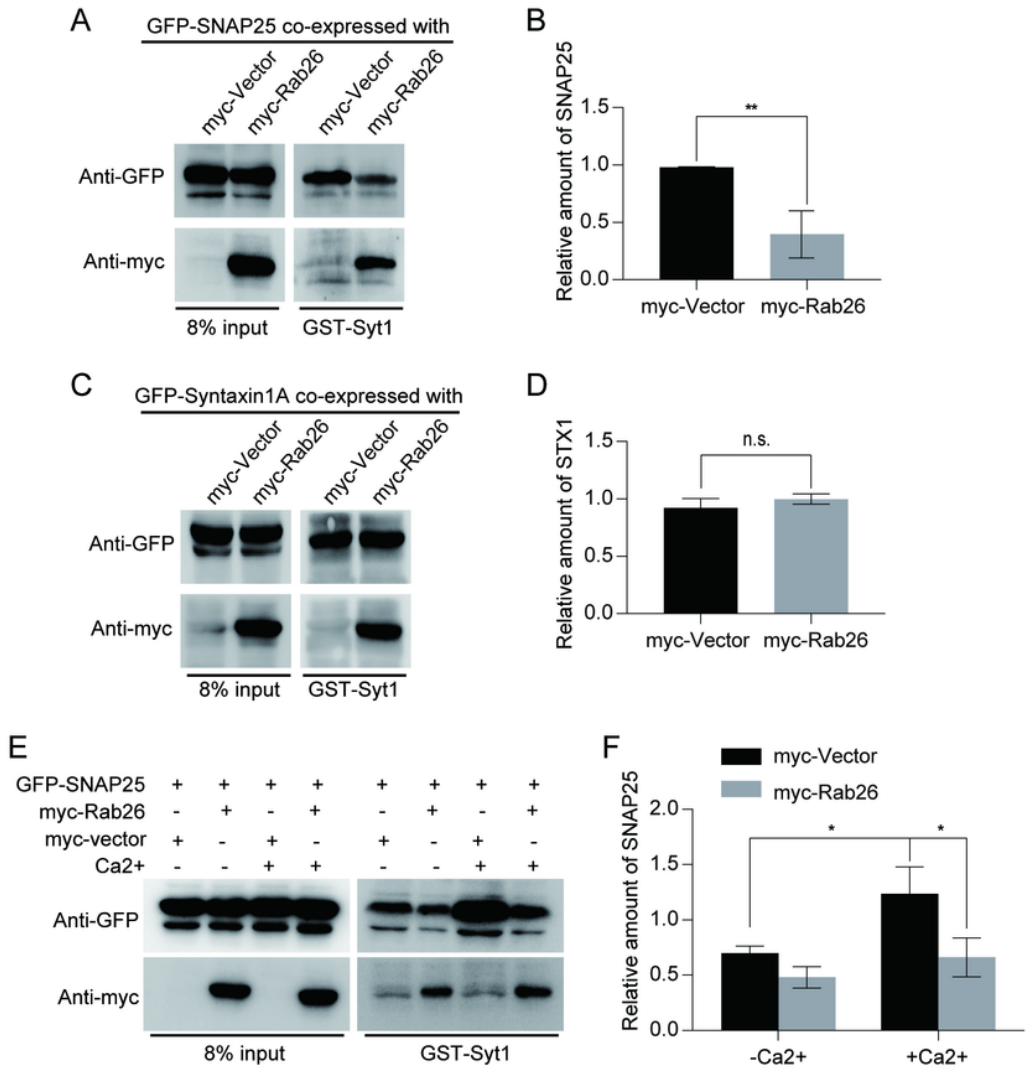

Figure 7

Rab26 influences the interaction between Syt1 and SNARE complex. (A), 293t cells were co-transfected myc-Vector and GFP-SNAP25 as control group, myc-Rab26 and GFP-SNAP25 as experimental group, incubated overnight with GST-Syt1 beads at 4°C through GST-pull down experiment, washed by lysis buffer, and analyzed by Western blotting with GFP antibody. And (B), Quantitative analysis of the results of A from three independent experiments. (C), 293t cells were transfected myc-Vector and GFP-Syntaxin

1A as control group, myc-Rab26 and GFP-Syntaxin 1A as experimental group, incubated with GST-Syt1 beads, and analyzed by Western blotting with GFP antibody. And (D), Quantitative analysis of the results of C from three independent experiments. (E), (A) Cells were incubated for 5min at 37°C in the presence of Ca^{2+} (10uM CaCl2) or absence of Ca^{2+}, indicating Rab26 reduces the interaction between Syt1 and SNAP25. (F), Quantitative analysis of the results of E from three independent experiments. (n=3; NS, not significant, ***P < 0.001, **P < 0.01, *P < 0.05, t-tests)

Figure 8

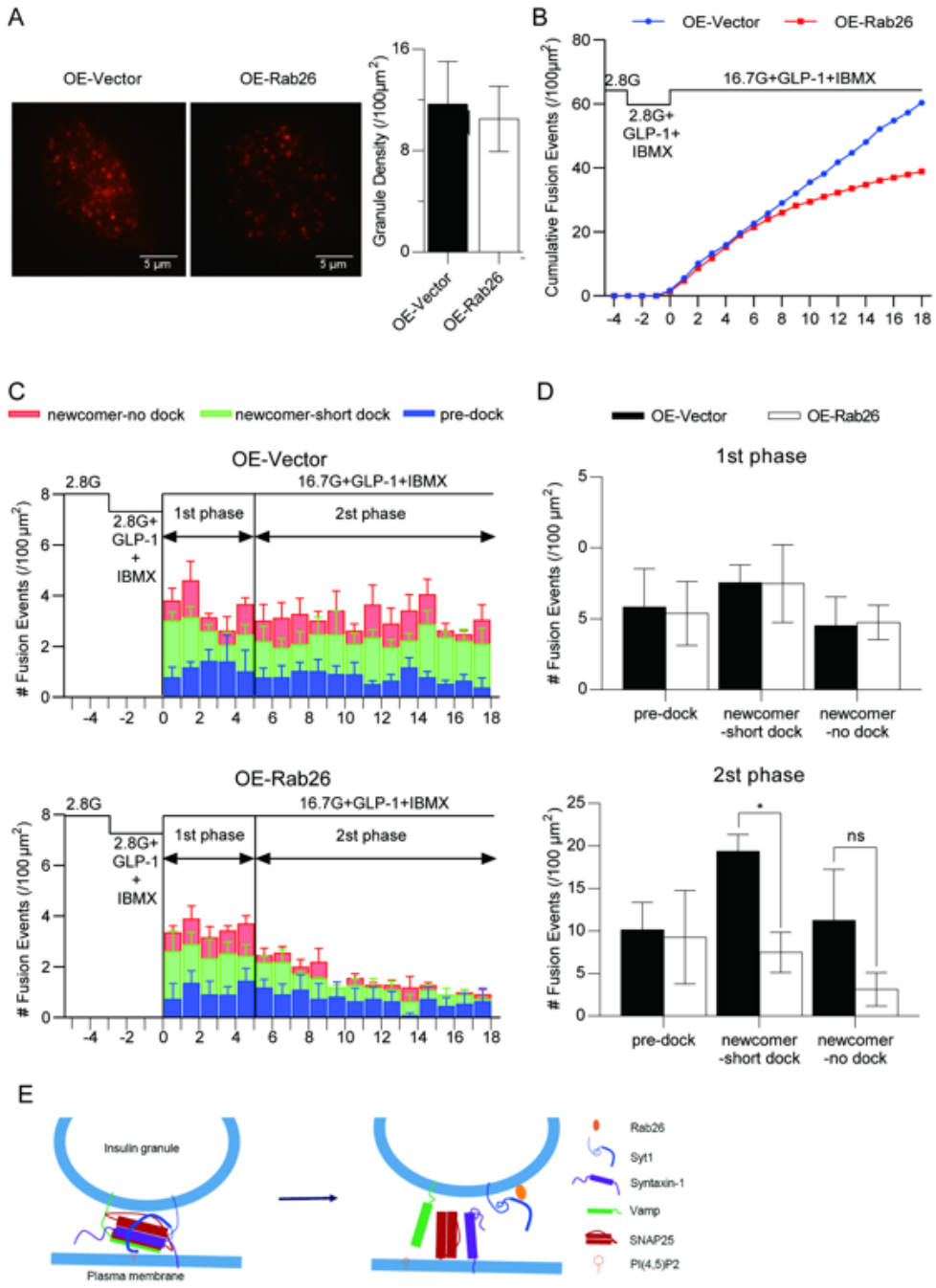

Figure 8

Rab26 inhibits exocytosis of newcomer insulin granules

(A) TIRF images of docked insulin granules in vector-transfected (OE-Vector) or Rab26-transfected (OE-Rab26) MIN6 cells, there is no significant difference in the averaged SG densities before stimulation. Data was collected from 3 experiments, and 3 cells were analyzed in each experiment, shown as means±SEMs.(B) Normalized cumulative fusion events of insulin granules per 100μm^2 from OE-Vector and OE-Rab26 MIN6 cells. (C) The insulin SGs exocytosis dynamics evoked by 16.7mM glucose from OE-Vector versus OE-Rab26 MIN6 cells. Data were obtained from 3 experiments and 3 cells were analyzed in each experiments, shown as means±SEMs. Blue, green and red bars indicate the insulin granules pre-dock, newcomer-short dock and newcomer-no dock, respectively. (D) Summary of the fusion events from three modes: pre-dock, newcomer-short dock and newcomer-no dock in the first phase and second phase after 16.7 mM glucose stimulation. (E), A model proposes Rab26 interacting with Syt1 to sequester it from promoting the formation of SNARE complex involved in the docking and fusion of insulin granules

Supplementary Files

This is a list of supplementary files associated with this preprint. Click to download.

- supplementaldata.pdf